Title

EFFECTS OF LIQUID AND SURFACE CHARACTERISTICS ON OSCILLATION BEHAVIOR OF DROPLETS UPON IMPACT

Journal

Atomization and Sprays, 24(10)

ISSN

1044-5110

Authors

Banks, Darren
Ajawara, Cynthia
Sanchez, Rafael
et al.

Publication Date

2014

DOI

10.1615/atomizspr.2014007590

Peer reviewed

Atomization and Sprays, 24 (10): 895–913 (2014)

EFFECTS OF LIQUID AND SURFACE CHARACTERISTICS ON OSCILLATION BEHAVIOR OF DROPLETS UPON IMPACT

Darren Banks, Cynthia Ajawara, Rafael Sanchez, Hamza Surti, & Guillermo Aguilar*

Department of Mechanical Engineering, University of California-Riverside, Riverside, California 92507, USA

*Address all correspondence to Guillermo Aguilar E-mail: gaguilar@engr.ucr.edu

Original Manuscript Submitted: 9/28/2013; Final Draft Received: 2/13/2014

The physical behavior of a single droplet impacting a surface is one of the most fascinating facets of spray research. Under some conditions, a droplet will strike and spread across a solid surface without splashing or rebounding. That droplet will spread and recoil for some time, oscillating between a disk and a hemisphere until these fluctuations diminish due to viscous damping. These oscillations affect the liquid coverage area and are essential in droplet solidification applications; yet little is known about them; Knowing more will, for example, enable higher-precision three-dimensional printing or enhanced droplet and spray cooling. Using mixtures of water and glycerol, oscillations of droplets with kinematic viscosities between 1.0×10^{-6} *and* 1.1×10^{-4} m^2/s *are explored, focusing on the damping behavior. Several impact substrates were used. Droplets freefall onto the target with velocities of 0.5–1.5 m/s. The Weber number of the droplets ranged from 10 to 100 and the Reynolds number from 15 to 4000. The impact velocity, spreading lamella diameter, and thickness at the center of each droplet were measured. Droplet kinematic viscosity, impact velocity, and surface tension effects are found to play a role in oscillations, which occur at approximately 75–90 Hz. For the liquids tested, a hydrophilic surface thins the droplet, arresting oscillations quickly, whereas a hydrophobic surface sustains oscillations. Correspondingly, a highly viscous droplet tends to stop oscillations sooner than a less viscous droplet. Increasing the velocity of impact restricts oscillations by spreading liquid across a larger area. For the range of conditions studied, viscosity dominates droplet oscillations when compared to the surface effects. We explore the interplay between viscous and surface tension effects in the oscillations. The spring constant and damping coefficient of an analogous harmonic system are calculated for the observed droplet oscillations. The tested liquid droplets generally exhibit underdamped behavior; higher damping coefficients are associated with more wetting and more viscous droplet liquids—a* 10^3 *increase in viscosity corresponds with an approximately* 10^1 *increase in damping. The spring constant appears to be influenced by the droplet composition and the surface wettability in a less trivial manner, with similar magnitudes and no discernable pattern in the spring constant (1.5–3.0 N/m) for all droplets and surface conditions examined.*

KEY WORDS: *droplet impact, wettability, oscillations, contact angle*

NOMENCLATURE

c	damping coefficient	d	dynamic
d	diameter of the droplet	D	drop
k	spring constant	L	lamella rim
m	characteristic mass	s	static/resting
t	thickness	T	treated with hydrophobic coating
U	impact velocity		
x	deflection		
Θ	contact angle	**Dimensionless Groups**	
σ	surface tension	Ca	$\mu U/\sigma$, capillary number
ρ	density	Fr	$U/\sqrt{gd}$, Froude number
ν	kinematic viscosity	Oh	$\mu/\sqrt{\rho\sigma d}$, Ohnesorge number
Subscripts		Re	Ud/v, Reynolds number
C	lamella center	We	$\rho U^2 d/\sigma$, Weber number

1. INTRODUCTION

Single-droplet impacts are the fundamental building block of a complete understanding of spray behavior. Much study has been done on impact phenomena, on dry as well as liquid surfaces. Six possible outcomes of a single droplet striking a dry surface have been defined; deposition, prompt splash, receding breakup, partial rebound, and complete rebound of the droplet all can occur, depending on droplet and surface properties and impact characteristics (Rioboo et al., 2001). For all outcomes, the focus of study has been on behaviors occurring just at or after impact. Prompt splash is seen immediately on impact, corona splash and receding breakup usually occur during the initial spreading, and rebound behavior occurs at the end of the first withdrawal. In some cases, however, the droplet impacts, spreads, recedes, and then continues to oscillate as motion is arrested by viscous and surface effects. The behavior during the later oscillations is often not as relevant to single-droplet impact phenomena; however, the delayed oscillations determine the surface the next droplet in a spray strikes, and thus merit examination.

Droplet impacts on hydrophilic and hydrophobic surfaces lead to interesting phenomena. Hydrophobic surfaces tend to increase the likelihood of splashing; as the spreading edge of the droplet is repulsed from the surface, instability based on density and acceleration differences between the liquid and ambient gas are magnified (Vu et al.,

2011). On a surface with both hydrophobic and hydrophilic regions, if a portion of a droplet spreads over a hydrophilic region, the droplet can migrate entirely to that region to minimize surface energy (Mock et al., 2005). Super-hydrophobic (nonwettable) substrates and very high fluid surface tension lead to repeated rebound "bouncing" behavior of droplets (Okumura et al., 2003). The effects of surface wettability on spreading and receding are explored, and the dynamic contact angle during postimpact oscillations has been measured in light of several dynamic wetting theories. One hydrodynamic wetting theory is found to work well during the initial spreading phase immediately after impact, but no expression could be found to describe the interaction of contact line movement and contact angle (Bayer and Megaridis, 2006). In this study, the focus is on low-Weber-number impacts ($10 < \mathrm{We} < 100$), with attention to the effects of elevated droplet viscosity. The low-Weber-number impacts were chosen to maximize oscillation behavior; at higher impact Weber numbers, it was found that oscillations were significantly diminished, possibly due to the droplet liquid spreading farther across the surface.

Noblin et al. (2004) studied induced oscillations of a droplet resting on a solid substrate, with a focus on the transition between a static contact line and a moving one (Noblin et al., 2004). Using a modified loudspeaker to vibrate an initial quiescent drop, the transition between an oscillating and a pinned contact line was investigated in light of the frequency and magnitude of the driving oscillations (Noblin et al., 2004). The experimental techniques and vibrational analysis performed by Noblin et al. are similar to the work presented in this paper, except that the focus of this paper is on impacting droplets and unforced oscillations, in contrast to deposited droplets and driven vibrations.

Our goal is to provide better understanding of the oscillations and spreading behaviors during droplet impacts, which will lead to improved control of droplet impact heat transfer. The thermal effects of droplet impacts onto liquid films depend on the film thickness (Vu et al., 2009); the oscillations of droplets regulate the thickness of liquid that subsequent droplets strike. The splashing behavior of single-droplet impacts depends on the target film thickness, as well—very thin films are more likely to lead to splashing than thicker films (Vander Wal et al., 2006). Understanding the behavior of the droplet long after impact is critical to applications in some methods of 3D printing, where droplets are sprayed in layers and solidify into controlled shapes (Martin et al., 2008).

2. EXPERIMENTAL METHODS

The goal of the experiment was to measure the amplitude and frequency of droplet oscillations. To that end, a high-speed video camera records the impact and subsequent oscillations. During the oscillations, the thickness of the liquid at the center of the splat was measured over time. The measured maximum and minimum thicknesses give the amplitude of oscillations; the mean of the spacing between successive maxima was used to determine the frequency.

Figure 1 shows the experimental setup. A microliter valve (EFI, Inc., model 740V-SS) driven and fed by air pressure dispenses liquid into a stainless steel nozzle of outer diameter 1.65 mm. The droplet grows on the end of the nozzle and detaches as gravity overcomes surface tension, freefalling onto the target substrate. Water and glycerol have similar values of surface tension and density, so the droplets detach from the nozzle at similar sizes: 3.3 ± 0.2 mm diameter. Droplets more than 0.1 mm larger or smaller than the mean were rejected. The height of the nozzle determines the time in freefall and thus the impact velocity. Nozzle height was varied from 0.6 to 10 cm to give a range of impact velocities from 0.5 to 1.5 m/s. A high-speed video camera (Phantom V7.1 with a Micro-Nikkor 105 mm lens) recorded impacts from the side. Recordings were taken at 800×600 pixel resolution at 5000 fps, captured using Phantom Camera Control software. The outer diameter of a bolt was measured using calipers (accuracy ± 0.01 mm), and the corresponding width was measured on video to give the length resolution of 0.010 mm/px at the focal distance of the camera lens. Velocity measurements are performed using sequential frames: the distance moved between two frames can be measured using the known pixel-to-distance ratio, and the time gap between the frames is known. Using the video to measure objects of known dimensions reveals less than 1% error in length measurements by this method; velocity measurement should have a slightly larger error due to blurring. The exposure time is set to 20 μs and a digital sharpening effect is applied; however, some blurring is inevitable.

Three substrate conditions were used: aluminum, hydrophilic coating on Teflon, and hydrophilic coating on acrylic. Each substrate was machined for smoothness to a tolerance <0.02 mm, making surface roughness 2 orders of magnitude smaller than the

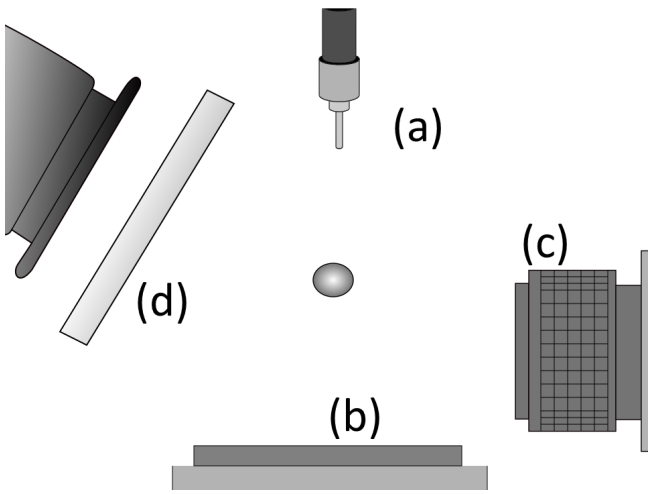

FIG. 1: Experimental setup: (a) the drop generator, positioned a known height above (b) the target surface; (c, d) high-speed video camera and diffused backlighting, respectively.

droplet diameter. Coatings are Rain-X brand rain repellant automotive windshield spray for the hydrophobic case and Rain-X Anti-fog for the hydrophilic case. Droplets were formed from deionized water, 60% by weight aqueous glycerol and 85% by weight aqueous glycerol. These droplets give a range of Weber numbers of 10–100 and Reynolds numbers of 15–4000, based on impact velocities of 0.54 ± 0.01 m/s for examining the effects of fluid properties and surface conditions, and 0.54–1.5 m/s when investigating the effect of impact velocity. After each droplet, the surfaces were cleaned, and if applicable, recoated with their treatments. Table 1 shows the static contact angle for each fluid on each surface, while Table 2 lists the relevant physical properties of each fluid.

Using high-speed video recordings, the impact velocity, dynamic contact angle, and spreading diameter are all measured during and immediately after the impact as a function of time. Figure 2(a) illustrates the positions of measurement of each of these quantities; Fig. 2(b) shows a series of still frames of typically observed droplet impacts and the first oscillation after impact.

An interesting note about Table 1 is the inverse reaction of the static contact angle of glycerol and water on various surfaces. On the hydrophobic-treated Teflon surface, increasing the percentage of glycerol decreases the contact angle. However, on every other surface, the contact angle increases with the proportion of glycerol.

Also of note is that the untreated acrylic and Teflon static contact angles were measured and are noted for reference, but experimental data is only taken on the treated surfaces. Our measurements of the contact angle on each untreated surface are very similar, so the treatments were applied to further differentiate them.

TABLE 1: Static and (average dynamic) contact angles of droplets on varied substrates

Fluid	Surface aluminum	Hydrophilic treated acrylic	Acrylic	Hydrophobic treated Teflon	Teflon
Water	10° (58°)	29° (51°)	37°	75°(87°)	35°
60% glycerol	17°	48° (44°)		64°	
85% glycerol	35°	54° (59°)	45°	66°	55°

TABLE 2: Fluid properties

Fluid	Density (g/cm^3)	Viscosity (cm^2/s)	Surface tension (dyne/cm)
Water	1.00	0.01	72.8
60% glycerol	1.15	0.09	66.9
85% glycerol	1.22	0.89	65.1

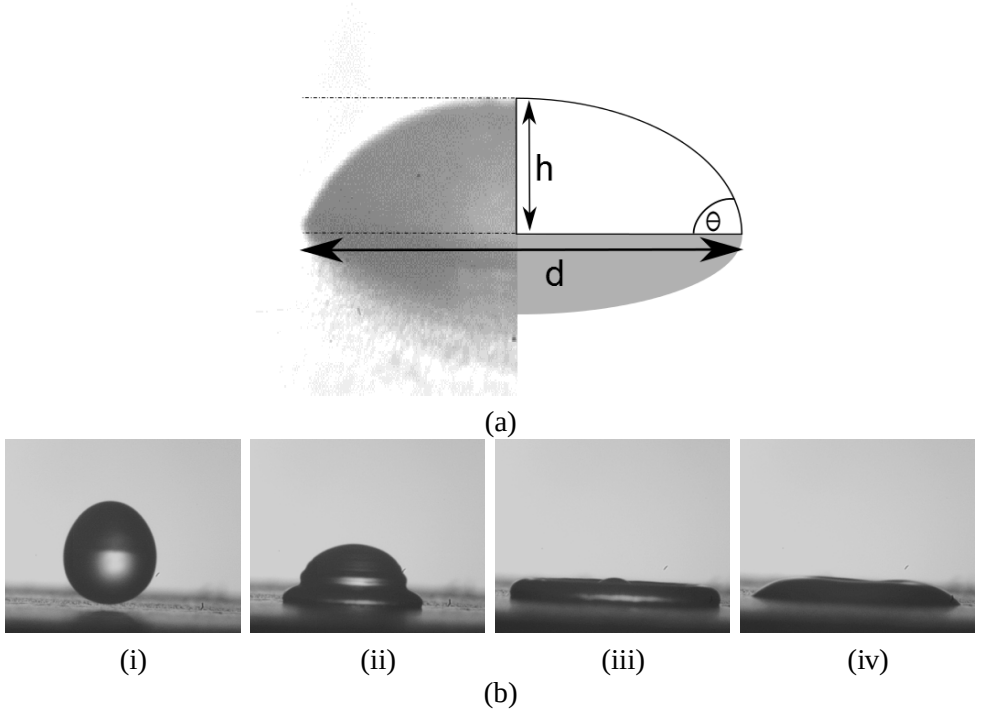

FIG. 2: (a) Measurement of contact angle and drop center thickness and (b) sequence of droplet oscillations: (i) 425 μs prior to impact; (ii) 1915 μs after impact, initial spreading; (iii) 6596 μs after impact, maximum spreading; and (iv) 12,765 μs after impact, receding.

3. EXPERIMENTAL RESULTS

3.1 Oscillations of Dynamic Contact Angle vs Splat Thickness

The effect of surface wettability on droplet oscillations, with all other characteristics remaining constant, was the first topic of study. Videos of a water droplet striking the aluminum, hydrophilic treated acrylic, and hydrophobic treated Teflon were taken. Figure 3 shows the dynamic contact angle and thickness of the water droplet as a function of time on each surface. The dynamic contact angle changes as the droplet oscillates. When the droplet is narrowest, the fluid tries to spread radially, increasing the contact angle; as the droplet recoils, the fluid moves inward, reducing the contact angle.

3.2 Viscosity and Wettability's Influence on Oscillations

Viscosity was shown to have a dramatic impact on droplet oscillation behaviors. By varying glycerol content in aqueous mixtures, the viscosity can be changed dramatically

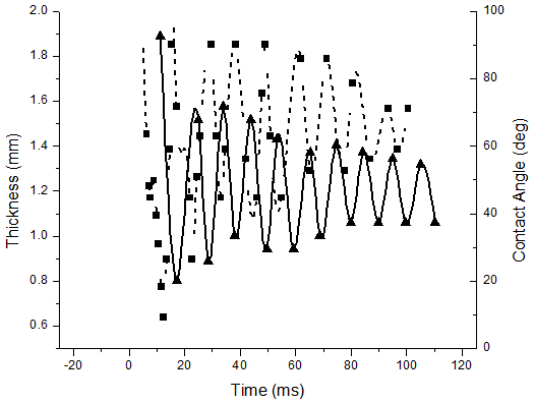

(a)

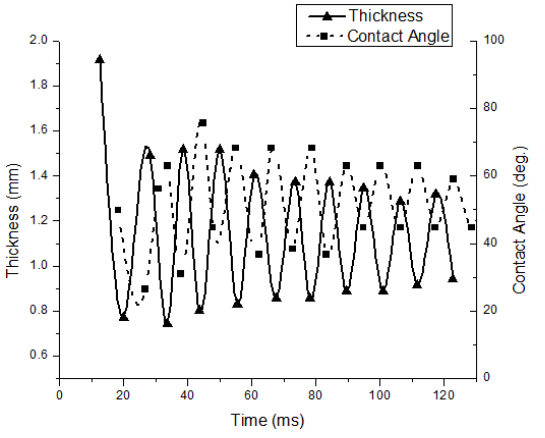

(b)

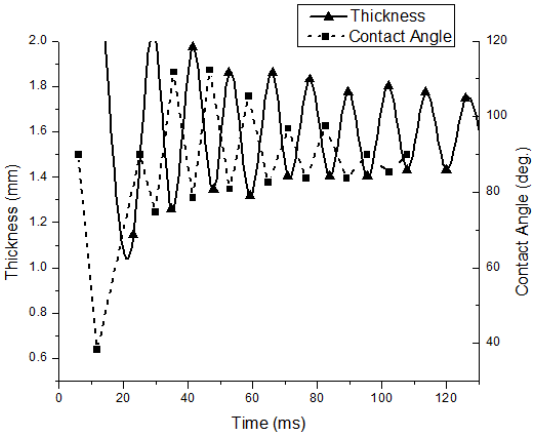

(c)

FIG. 3: Dynamic contact angle of a water droplet oscillating on varying substrates: (a) aluminum substrate, (b) acrylic substrate, and (c) Teflon substrate.

without significantly affecting other fluid properties, as seen in Table 2. Differing-fluid droplets were recorded striking the treated acrylic surface, which is the intermediate surface on the range of wettability. Figure 4 shows the dynamic contact angle and oscillations over time for the range of fluids studied on the acrylic surface. Figures 3 and 4 show that the dynamic contact angle varies at approximately the same frequency but are generally opposite in phase to the center thickness for water droplets on all three surface conditions and for each droplet fluid on the acrylic surface. The average dynamic contact angle is generally larger than the corresponding static one (Table 1). The reason for this is that the resting liquid shape is hemispherical, which corresponds to the lower ranges of dynamic contact angle.

Figure 5 shows the center thickness over time for all droplets oscillating on the aluminum surface, and Fig. 6 the same on the hydrophobic treated Teflon surface. Using the average of the peak-to-peak time, the frequency can be calculated from the data presented in Figs. 4–6. Table 3 lists the frequencies measured for each droplet and surface combination. The surface condition has varying effects on the frequency for each of the three droplet fluids. For water, the hydrophobic surface (Teflon) produces the lowest frequency (80 Hz). As the surface grows more hydrophilic, the droplet oscillates faster, reaching 96 Hz on aluminum. However, the opposite effect is observed for droplets composed of 60% glycerol—the droplet oscillates fastest on the more hydrophobic surface and decreases in frequency for more hydrophilic surfaces. The frequencies of oscillation of 85% glycerol droplets seem to ignore the surface conditions—the measured frequencies on all three surfaces vary by approximately 1 Hz.

Both viscosity and wettability seem to affect postimpact oscillations, but viscosity seems to have the larger effect over the range of conditions studied. The differences in oscillation amplitude and duration between surfaces for any of the three droplet fluids are much smaller than the corresponding differences between the droplet fluids. Water, having the lowest viscosity, shows the largest amplitude ($\sim \pm 0.4$ mm initially on all three surfaces) and the most sustained oscillations out of all three droplet fluids (lasting in excess of 120 ms), visible in Fig. 3. The 60% glycerol droplets have reduced initial amplitude ($\sim \pm 0.3$ mm) and oscillations die off before 120 ms. Increasing viscosity further with 85% glycerol droplets leads to initial amplitude of only $\sim \pm 0.1$ mm and no oscillations after only 50 ms, on all surface conditions in this study. In contrast, the differences in initial amplitude between surfaces for each fluid are minimal, on the order of 0.02 mm variation. The surface condition does seem to play a role in the duration of measurable oscillations. For all three droplet species, oscillations die off most quickly on aluminum. The last measurable oscillation occurs 15–25% sooner on aluminum than on the other surfaces for each of the droplet liquids.

On the hydrophobic treated Teflon surface, all three droplet liquids have the highest mean of their oscillations. On that surface, the mean is inversely related to viscosity—water has the largest mean value and 85% glycerol the smallest. Interestingly, on the other two surfaces, 85% glycerol has a higher mean thickness than 60% glycerol. This

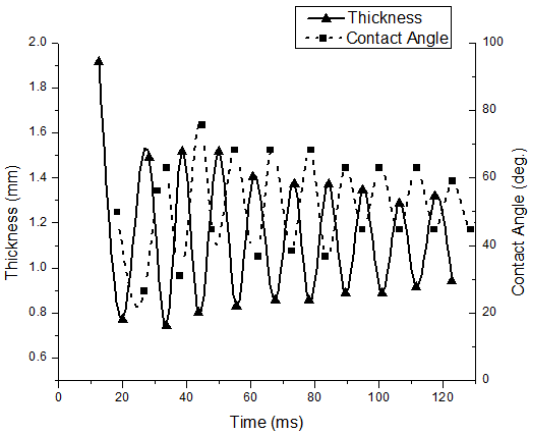

(a)

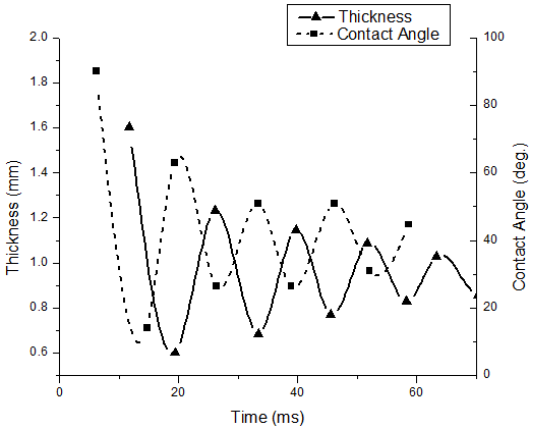

(b)

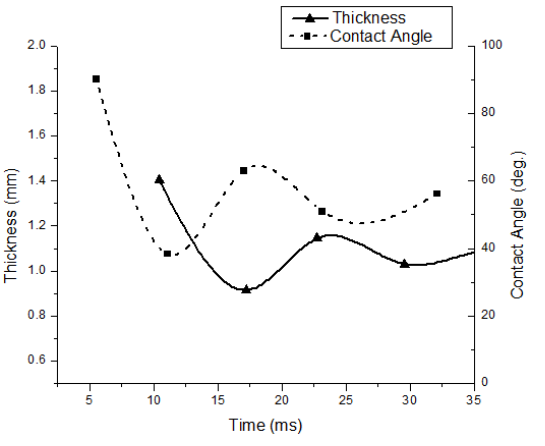

(c)

FIG. 4: Dynamic contact angle and thickness of varying-viscosity drops oscillating on treated acrylic: (a) water droplet, (b) 60% glycerol droplet, and (c) 85% glycerol droplet.

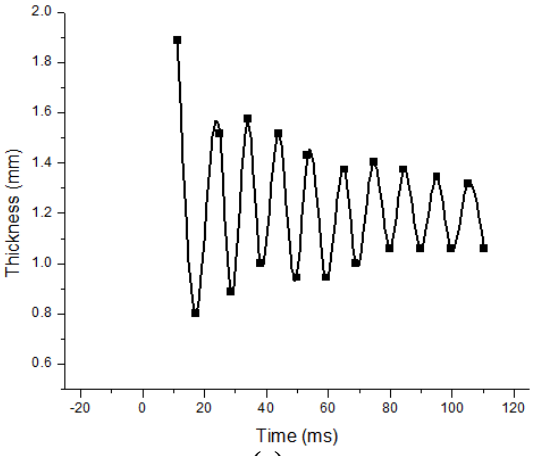

(a)

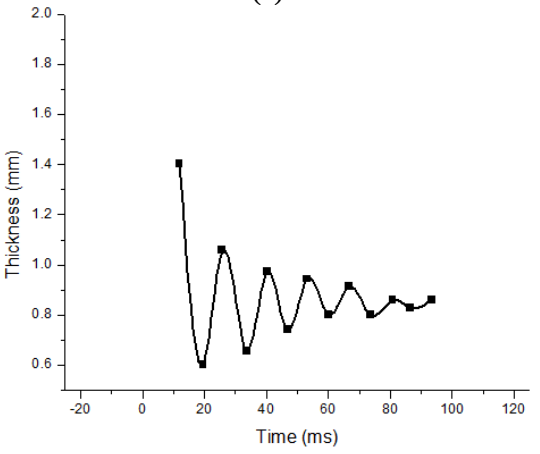

(b)

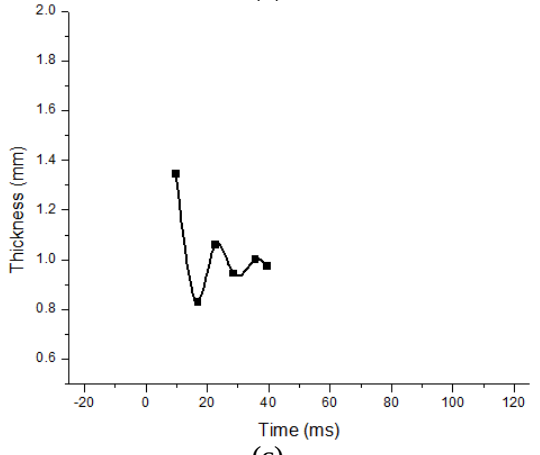

(c)

FIG. 5: Center thickness of various drops oscillating on an aluminum substrate: (a) water droplet, (b) 60% glycerol droplet, and (c) 85% glycerol droplet.

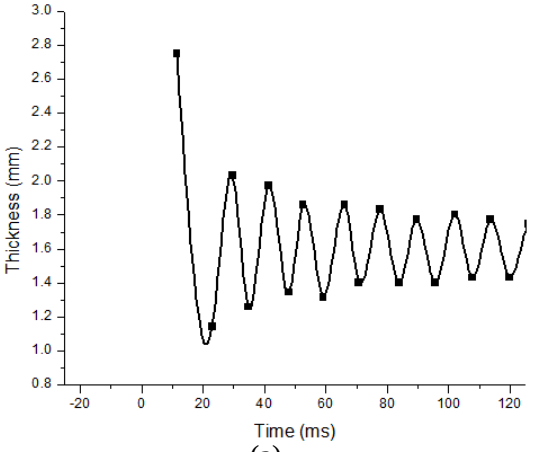

(a)

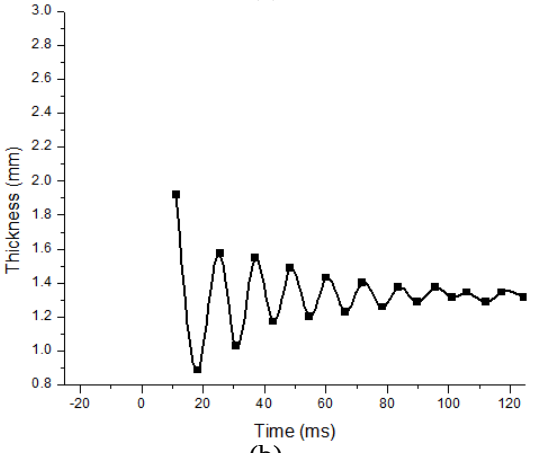

(b)

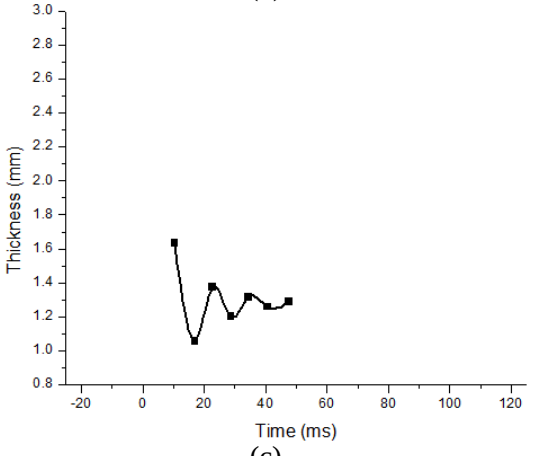

(c)

FIG. 6: Center thickness of various drops oscillating on hydrophobic treated Teflon: (a) water droplet, (b) 60% glycerol droplet, and (c) 85% glycerol droplet.

TABLE 3: Frequency of oscillation of each droplet on each surface, given in Hz

Fluid	Surface aluminum	Hydrophilic acrylic treatment	Hydrophobic Teflon treatment
Water	96	87	81
60% glycerol	74	79	85
85% glycerol	83	84	83
Water, 0.57 m/s			57
Water, 0.81 m/s			42

suggests that as the surface grows more hydrophilic, viscosity plays a larger role in restricting the droplet spreading, similar to the thicker spreading lamella effect observed by Vu et al. (2011) for high-viscosity droplets. Furthermore, the interaction of glycerol with the surface treatments may influence how the droplets spread. However, when considering the differences observed in oscillation frequency and amplitude, it seems probable that viscosity is the dominant factor in controlling droplet spreading in these cases.

3.3 Velocity's Influence on Oscillations

Finally, the oscillations of a water droplet after striking a Teflon surface at varying impact velocities were measured over a range of 1.07–1.62 m/s ($50 < \mathrm{We} < 140$). Impact velocity was found to play a role in the amplitude, frequency, and mean value of oscillations. Higher impact velocity reduced the amplitude of oscillations, lowered the frequency, and decreased the mean value of the thickness of the droplet. Figure 7 shows the oscillations of a water droplet that impacted a treated Teflon surface at 1.07 and 1.34 m/s. The droplets that impacted at higher velocities did not oscillate measurably. The higher-velocity droplets spread thinner initially but then oscillate and retract, leading to a mean of oscillation that grows over time.

Increased velocity reduced the amplitude and mean thickness of the droplet for a very simple reason. As the velocity increased, the radius of the droplet when the contact line stopped moving increased correspondingly. The volume of the droplet is virtually identical in each case, so the larger radius results in a droplet that is thinner on average and has less vertical freedom to oscillate. Further, the larger radius means the wavelength of motion in the droplet is longer, leading to an observed decrease in frequency. Similar reasoning may apply in the case of hydrophilic vs hydrophobic surfaces—both water and 85% glycerol each have higher frequencies and higher amplitudes as the surfaces get more hydrophobic, leading to a smaller pinned contact line diameter and thus thicker volume and shorter wavelength. As the velocity increases, the drop spreads further across the substrate, until the kinetic energy of the impact has been lost. At that point, the

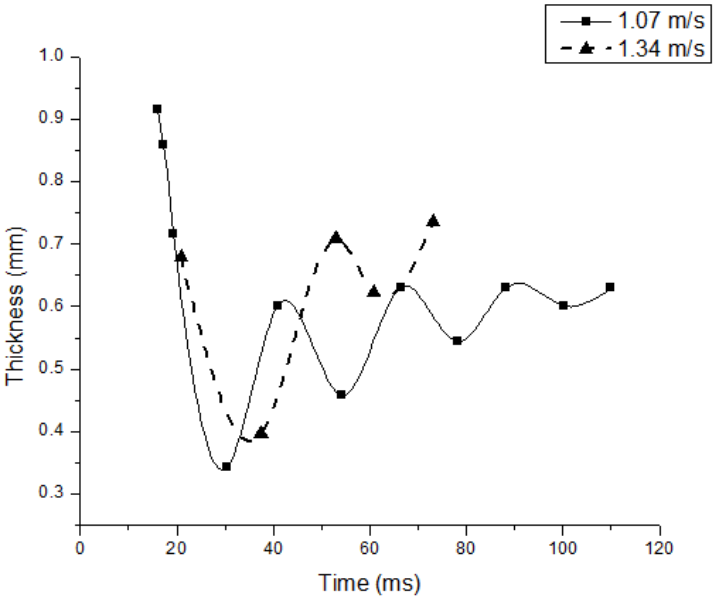

FIG. 7: Center thickness of water drops oscillating after impact at varying velocities.

surface tension is the only cause of flow, leading to a gradual, nonoscillating retraction of the droplet into a hemisphere.

3.4 Vibration Analogy

The behavior of a liquid droplet after impact was compared to a damped harmonic oscillator. If x is the deflection from a neutral state, k is a spring constant, c is a damping coefficient, and m is the mass of the system. The motion of an unforced harmonic oscillator is represented by Eq. (1), assuming there is no force driving the vibrations (Thomson and Dahleh, 1998):

$$m\ddot{x} = -kx - c\dot{x} \tag{1}$$

This differential equation has an exponentially decaying solution (Thomson and Dahleh, 1998):

$$x(t) = \exp\left(-\frac{c}{2m}t\right)\left[A\exp\left(\sqrt{\left(\frac{c}{2m}\right)^2 - \frac{k}{m}}t\right) + B\exp\left(-\sqrt{\left(\frac{c}{2m}\right)^2 - \frac{k}{m}}t\right)\right] \tag{2}$$

In Eq. (2), if an oscillator is "underdamped," the terms within the radicals will be imaginary and the equation can be reformulated in terms of trigonometric functions:

$$x(t) = \exp\left(-\frac{c}{2m}t\right)\left[A\cos\left(\sqrt{\frac{k}{m} - \left(\frac{c}{2m}\right)^2}t\right) \pm B\sin\left(\sqrt{\frac{k}{m} - \left(\frac{c}{2m}\right)^2}t\right)\right] \tag{3}$$

Qualitatively, underdamped oscillations are apparent in all of the observed water and 60% glycerol droplet impacts, so oscillations are sustained for many cycles. In contrast, the oscillations of the highly viscous 85% glycerol droplets are more qualitatively overdamped; quiescence occurs after very few oscillations.

In the context of a droplet oscillating on a surface, we hypothesize viscosity ought to play a role primarily in the damping coefficient, c; viscosity will remove energy from the oscillating fluid, acting to diminish the amplitude of the oscillation over time. The spring constant in Eq. (1), k, is related to how strongly the oscillating system pulls itself toward a neutral state. The surface tension and interactions between the droplet and the surface are what we hypothesize to principally drive the recoiling action of a droplet; as such, k ought to depend on them with limited or no dependence on viscosity.

Using the exponential term in Eq. (3), the value of c can be computed. That exponential term, when plotted alongside the oscillations, will follow the peaks of the oscillations, as shown in Fig. 8. By fitting an exponential curve of the form $A*\exp(-b*t)$ to the peaks of the oscillations, the power of the fitted curve (b) can be compared to the value $-c/2m$. Table 4 lists the computed damping coefficients, and Fig. 8 plots the oscillations of a water droplet on the acrylic surface, with the exponential damping curve plotted alongside.

Correspondingly, the spring constant can be determined by equating the experimentally determined frequency to the frequency term in Eq. (3). The factor of 2π converts the frequency to radians/second.

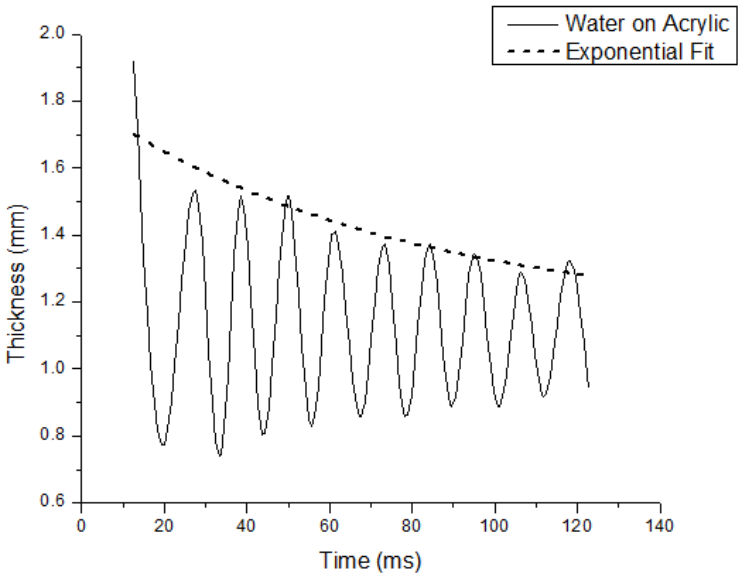

FIG. 8: Exponential fitting to the peaks of the oscillations of a water droplet on an acrylic surface.

TABLE 4: Damping coefficients (c) of droplets onto each surface, given in N s/m

Fluid	Surface aluminum	Treated acrylic	Treated Teflon
Water, 0.45 m/s	2.50×10^{-4}	2.23×10^{-4}	2.92×10^{-4}
60% glycerol, 0.45 m/s	7.50×10^{-4}	8.96×10^{-4}	5.36×10^{-4}
85% glycerol, 0.45 m/s	1.95×10^{-3}	1.47×10^{-3}	1.35×10^{-4}

$$2\pi f = \sqrt{\frac{k}{m} - \left(\frac{c}{2m}\right)^2} \tag{4}$$

Rearranging Eq. (4) to find the spring constant:

$$k = m\left[(2\pi f)^2 + \left(\frac{c}{2m}\right)^2\right] \tag{5}$$

Table 5 lists the calculated spring constants for each droplet. That table also contains "best-fit" spring constants. The calculated spring constants do not always fit the observed droplet oscillations very well. To find the best-fit constants, Eq. (3) was plotted using the damping coefficient from the exponential fit and k calculated from Eq. (5). If the RMS error between the predicted and the measured oscillations was larger than 10%, the spring constant was adjusted in increments of 0.01 N/m until the RMS percentage error between the measured and predicted oscillations was below 10%. Figure 9 depicts the measured and predicted oscillations of a 60% glycerol droplet impacting an acrylic surface, a case for which the calculated spring constant qualitatively accurately predicted the oscillations (RMS = 4.2%). Figure 10 depicts the measured, predicted, and best-fit spring constant for the 85% glycerol droplet on an acrylic surface. The small increment in spring constant greatly improves the agreement between the measured and predicted curves—RMS error drops from 49% to 9.3%.

This inaccuracy appears to derive from small asymmetry in the droplet's oscillations. Many times the droplet would oscillate off-center from the point of impact, leading to irregular (fluctuating over time) frequencies. While droplets that visibly exhibited such

TABLE 5: Spring constants (k) of droplets onto each surface, given in N/m. The first number is the frequency-predicted spring constant, and the second number is the best-fit spring constant, that is, the closest spring constant that results in an RMS error $<$10% between measurement and prediction.

Fluid	Surface aluminum	Treated acrylic	Treated Teflon
Water, 0.45 m/s	2.52/2.52	2.48/2.44	2.14/2.45
60% glycerol, 0.45 m/s	1.83/1.98	2.16/2.16	2.30/2.30
85% glycerol, 0.45 m/s	2.24/1.96	2.27/1.64	2.17/1.73

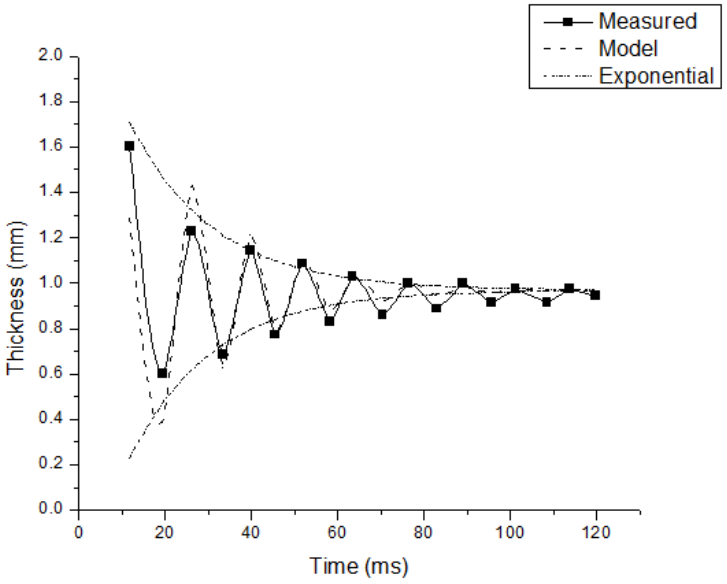

FIG. 9: Comparison of the measured data points, the damped-oscillation model, and the damping exponential curves.

behavior were rejected for measurement, there is likely to be some asymmetry in the oscillations. Even a small asymmetry causing a change in frequency would strongly appear in the spring constant. A future study may refine the droplet oscillation model to account for these asymmetries.

From Table 4, we observe that all droplets show higher damping coefficients on the more hydrophilic surfaces, in line with the findings discussed regarding Fig. 3. The increased viscosity of glycerol contributes to higher damping coefficients, with 85% glycerol having just under an order of magnitude larger damping coefficient than water on all three surfaces, and 60% glycerol approximately bisecting the other two liquids. A quick estimate suggests that the damping coefficient increases approximately following the square root of viscosity; however, a wider range of fluid would be necessary to verify this.

The spring constant does not seem to follow the same trends as the damping coefficient. For the acrylic and the Teflon surfaces, the spring constant is very similar for each of the droplet fluids—less than a 10% difference. This appears to support the hypothesis that the spring constant is related to the surface tension, as the droplet fluids all have very similar surface tensions. A future study will need to use fluids with different surface tensions to verify this. On aluminum, however, the spring constant seems to be influenced significantly by the droplet composition. Water is predicted to have nearly twice as large of a spring constant as 85% glycerol, and the best-fit spring constants are even farther apart.

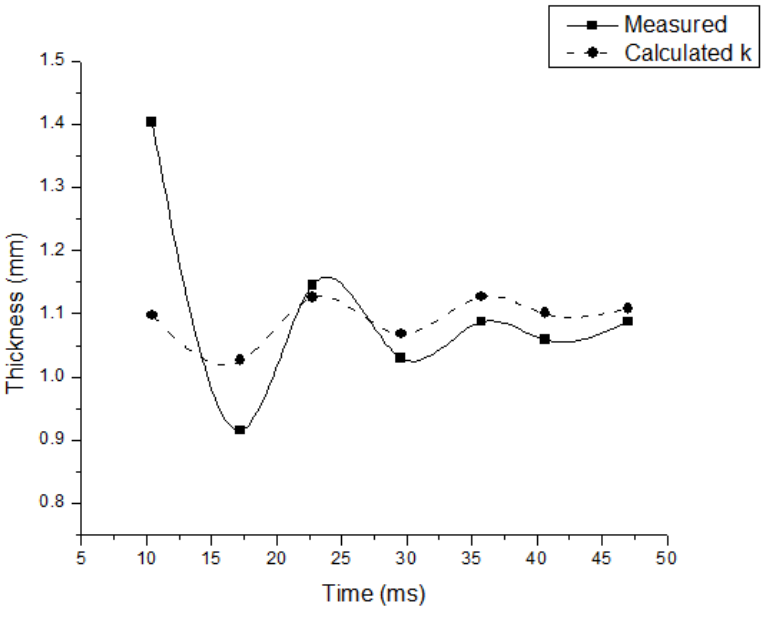

(a)

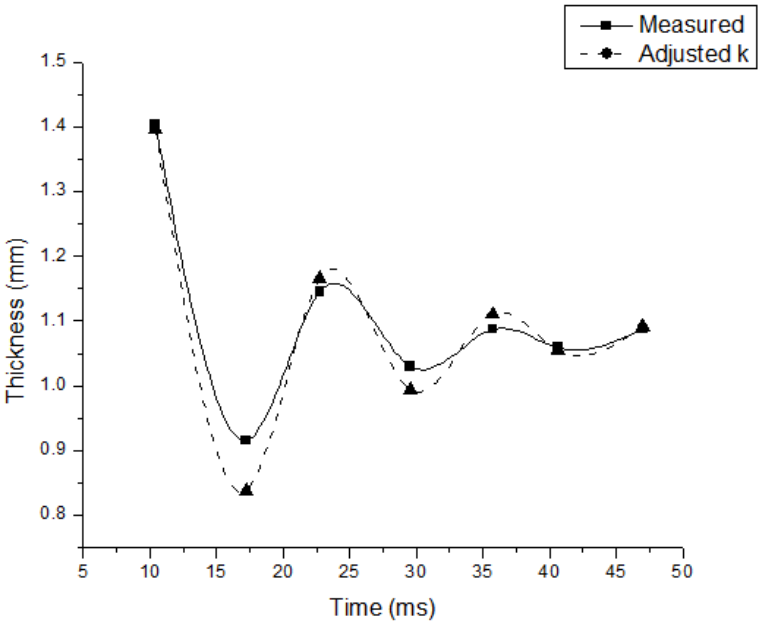

(b)

FIG. 10: Comparison of measured data points and predicted oscillation curves for 85% glycerol on an acrylic surface. The adjustment in the spring constant, k, is from 2.24 to 1.96 N/m, resulting in improved oscillation prediction (RMS error decreases 49% to 9.3%).

The higher-velocity water droplets did not follow the same fitting as the other cases because the oscillations were around an increasing mean. The exponential fit could not be used. However, the duration and amplitude of the oscillations can be commented on. Compared with the lower velocity water droplet impacting on the same surface, the increased velocity seems to result in more rapidly diminishing oscillation amplitude, suggesting a higher effective damping coefficient. At 120 ms after impact, for example, the low-velocity (0.55 m/s) case shows oscillations with amplitudes of approximately 0.2 mm above and below the mean. At the same time, after a 1.07 m/s impact, oscillations have faded to less than 0.05 mm around the mean. For a 1.34 m/s impact, the oscillations are too small to be measured at 80 ms after impact. The frequency, as well, is influenced by the impact velocity. The frequency of a low-velocity water droplet is 87 Hz; the 1.07 m/s droplet oscillates much slower, only 57 Hz, and the 1.34 m/s droplet oscillates at 42 Hz. The decrease in frequency suggests an analogous decrease in the spring constant for these droplets. However, the qualitative increase in damping coefficient may balance out the effect of the frequency change, as each influences the spring constant [Eq. (5)].

4. CONCLUSIONS

Measurements reveal that the mean of the dynamic contact angle scales with the static contact angle. Furthermore, hydrophobic surfaces lead to larger changes in dynamic contact angle than hydrophilic ones, suggesting hydrophilic surfaces restrict the droplet motion more effectively.

On all surfaces, the lowest viscosity water droplets show sustained large oscillations relative to higher-viscosity fluids—an intuitive result. Increasing viscosity damps oscillations severely. This damping can be qualitatively observed as reduced magnitude and duration of oscillations after impact. The higher-viscosity droplets oscillate less and come to rest more quickly than lower-viscosity ones.

Droplet oscillations seem to depend heavily on the radius of the droplet after the contact line has stopped moving. The magnitude of this radius determines the average thickness of the drop; the amount of vertical freedom the droplet fluid has while oscillating, governing the amplitude of oscillations; and the wavelength of motion that governs the oscillation frequency. Higher velocities and more hydrophilic surfaces lead to thinner, slower oscillating and more severely damped droplet motion. However, the sustaining effect of a hydrophobic surface is greatly outweighed by the damping effect of increased viscosity.

The analogy of droplet impact oscillations to damped harmonic oscillations has been made, with the spring constant and damping coefficient demonstrated to scale with droplet viscosity, surface tension, and velocity. Each of these factors appears to play an intertwined role in the analogy, but generally it can be said that increasing viscosity and velocity corresponds with increased damping and spring coefficients, while increasing

contact angles lead to higher damping and spring coefficients in water, and the reverse when the droplet is a glycerol mixture.

REFERENCES

Bayer, I. S. and Megaridis, C. M., Contact angle dynamics in droplets impacting on flat surfaces with different wetting characteristics, *J. Fluid Mech.*, vol. **558**, p. 415, 2006.

Martin, G. D., Hoath, S. D., and Hutchings, I. M., Inkjet printing—The physics of manipulating liquid jets and drops, *J. Phys. Conf. Ser.*, vol. **105**, pp. 1–15, 2008.

Mock, U., Michel, T., Tropea, C., Roisman, I., and Rühe, J., Drop impact on chemically structured arrays, *J. Phys. Condens. Matter*, vol. **17**, no. 9, pp. S595–S605, 2005.

Noblin, X., Buguin, A., and Brochard-Wyart, F., Vibrated sessile drops: Transition between pinned and mobile contact line oscillations, *Eur. Phys. J. E*, vol. **14**, no. 4, pp. 395–404, 2004.

Okumura, K., Chevy, F., Richard, D., Quèrè, D., and Clanet, C., Water spring: A model for bouncing drops, *Eur. Phys. Lett.*, vol. **62**, no. 2, pp. 237–243, 2003.

Rioboo, R., Tropea, C., and Marengo, M., Outcomes from a drop impact on solid surfaces, *Atomization Sprays*, vol. **11**, no. 2, pp. 155–165, 2001.

Thomson, W. T. and Dahleh, M. D., *Theory of Vibration with Applications*, Upper Saddle River, NJ: Prentice-Hall, Inc., 1998.

Vander Wal, R. L., Berger, G. M., and Mozes, S. D., Droplets splashing upon films of the same fluid of various depths, *Exp. Fluids*, vol. **40**, no. 1, pp. 33–52, 2006.

Vu, H., Aguilar, G., and Jepsen, R., Single droplet heat transfer through shallow liquid pools, *11th Intl. Conf. on Liquid Atomization Spray Studies*, Vail, CO, 2009.

Vu, H., Banks, D., and Aguilar, G., Examining viscosity and surface wettability in lamella lift dynamics and droplet splashing, *Atomization Sprays*, vol. **21**, no. 4, 2011.